

## SQUID-Based Bioassay with Magnetic Particles in Flow

M A Espy\*, C Carr, J H Sandin, C J Hanson, S G Daniels, A N Matlachov,  
S W Graves, M D Ward and R H Kraus, Jr

Los Alamos National Laboratory, Los Alamos, NM 87545, USA

S Fritz and D Leslie-Pelecky

CMRA, University of Nebraska-Lincoln, Lincoln, NE 68588, USA

\*corresponding author – espy@lanl.gov

**Abstract.** We present preliminary results for a magnetic flow spectrometer for magnetic microparticle separation, and a magnetic flow cytometer for particle identification. The application of the instrument is to high-throughput bioassay. Here we report on the first application of our magnetic spectrometer to the sorting of ferromagnetic and superparamagnetic microspheres in flow. The system is based on a permanent magnet quadrupole and separates the polymer coated magnetic microspheres based on their magnetic moments. The cryogenic section of our magnetic flow cytometer, which involves SQUID-based detection of the sorted magnetic microspheres based on their magnetic moments, has been re-engineered to permit a smaller standoff between the SQUID array and the flowing magnetic particles. We present preliminary results with the new experimental setup, with an emphasis on both spatial and signal resolution.

### 1. Introduction

The goal of bioassay is a highly parallel, high throughput and high sensitivity quantitative molecular analysis technique that can be used to expand current biomedical research capabilities. The use of superconducting quantum interference devices (SQUIDs) [1] or fluxgate magnetometers [2] in assay techniques is now common, with many recent developments utilizing nanoparticle relaxation as a key part of the process.

In this project we rely on somewhat larger particles ( $\sim\mu\text{m}$  diameter), and do not use the relaxation of particles, but instead their magnetic moment,  $M$ . In the first stage, each particle, which is generally spherical in shape, is separated into distinct populations defined by their magnetic moment. This is achieved by flowing the sample through a flow spectrometer that is placed in a quadrupole magnet. The quadrupole provides a linear magnetic field gradient, which deflects the magnetic microspheres an amount proportional to their magnetic moments, and the microspheres are then collected in different outlet bins in populations of similar magnetic moments. The next stage (not reported here) conjugates the magnetic particles with target molecules and finally, the sample is flown past optical and magnetic sensors, where the molecule can be identified (by the SQUID) by its magnetic moment.

### 2. Magnetic Particles

The intended material for our particles was to be samarium cobalt ( $\text{SmCo}_5$ ), a permanent magnet material with high coercivity and, more importantly for SQUID-based detection, a very high remanent magnetisation. Unlike using paramagnetic materials (which are common) the requirement for locating a magnet source near the particles while in would be obviated. The lack of literature available on  $\text{SmCo}_5$

nanoparticles is an indicator of the level of difficulty experienced in fabricating such particles. Initial production attempts revealed that particles (even when coated with carbon) quickly oxidised and thus their magnetic properties rapidly deteriorated. Work is ongoing at the University of Nebraska-Lincoln (UNL) to try and solve the problem of oxidisation and in the meantime, alternative particles are being used to perform “proof of principle” experiments.

Superparamagnetic particles require a magnetic field to exhibit a magnetic moment. This is the major difference between them and ferromagnetic particles discussed above. In principle, since we are using a strong field gradient to separate the magnetic particles, we could use superparamagnetic particles in the sorting portion of our experiment; the only downside would be that they would tend to deflect less in the gradient. For the second stage involving SQUID detection, if the particle relaxation time was sufficiently long (a few seconds), then we could place a magnet outside the cryostat and, by controlling the flow rate, detect the particles as they flowed under the SQUIDS.

We sourced both weakly ferromagnetic and superparamagnetic microspheres from commercial suppliers. The former were  $\text{CrO}_2$  with a mean diameter of  $8 \mu\text{m}$  [3] while the latter were  $\text{Fe}_3\text{O}_4$  with a mean diameter of  $10 \mu\text{m}$  [4]. We are also investigating the potential use of graphite coated iron particles, provided by UNL, with size ranges from  $5\text{-}100 \mu\text{m}$ . The advantage of using commercial samples is that they are monodisperse and have a size that allows us to count them in our laser-based fluorescence counter. However, the iron samples have a much higher saturation magnetization ( $54 \text{ emu/g}$  at  $2500 \text{ G}$ ).

### 3. Sorting of Magnetic Particles

Magnetic sorting takes place in a chamber  $16 \text{ cm} \times 2.2 \text{ cm} \times 0.5 \text{ cm}$ , shown schematically in figure 1(a). Surfactant is used in the chamber to reduce the effects of bubbles. A 10-channel syringe pump is used to draw sheath (and sample) from the outlets. In the absence of a field gradient all the particles (magnetic and non-magnetic) fall into bins 1 and 2 as expected. The chamber is located inside a quadrupole magnet, thus the gradient is linear and the trajectories for ferromagnetic particles are straight lines. In figure 1(b) we see the modeled deflection of the ferromagnetic  $\text{CrO}_2$  (Spherotech) and superparamagnetic  $\text{Fe}_3\text{O}_4$  (Bangs) microspheres. Figure 1(c) shows a histogram of particle count against bin number for an experiment using the same two sets of particles. There is good agreement with the predicted behavior, with the Spherotech beads hitting the wall and being entirely collected in bin 8, while the majority of the Bangs beads are collected in bin 4. The much larger iron particles from UNL (model and data not shown) were also predicted to hit the wall of the chamber and in qualitative experiments we do see a deflection in flow that is so marked that they move all the way across the chamber and only fall into bin 8 once the magnetic field

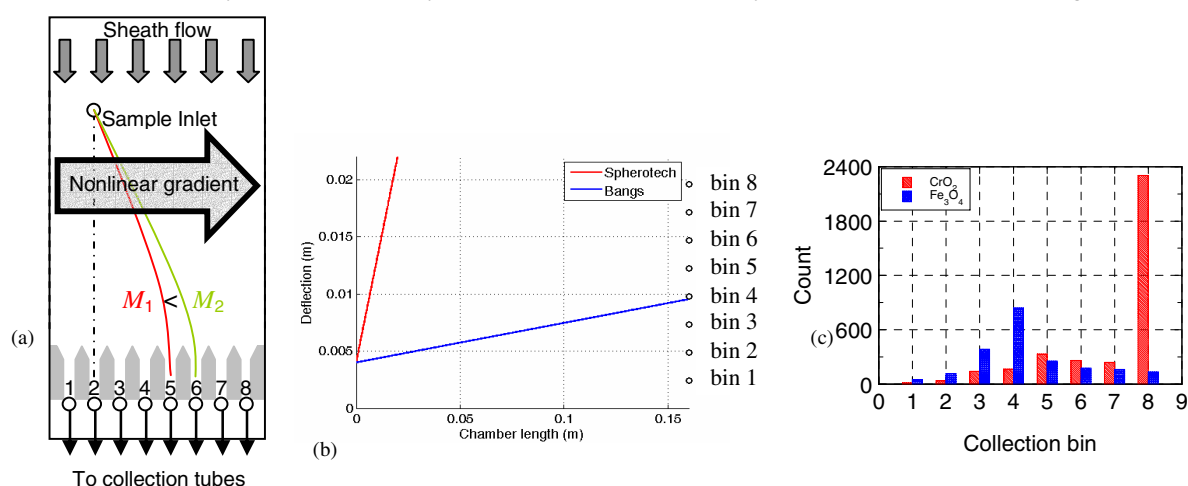


**Figure 1.** (a) Schematic representation of the principle behind the magnetic flow spectrometer. In (b) we have modeled the deflection of the particles given their size, magnetic properties, sheath flow rate, dimensions of the chamber and field gradient, while in (c) we have collated the available particle count data in a histogram.

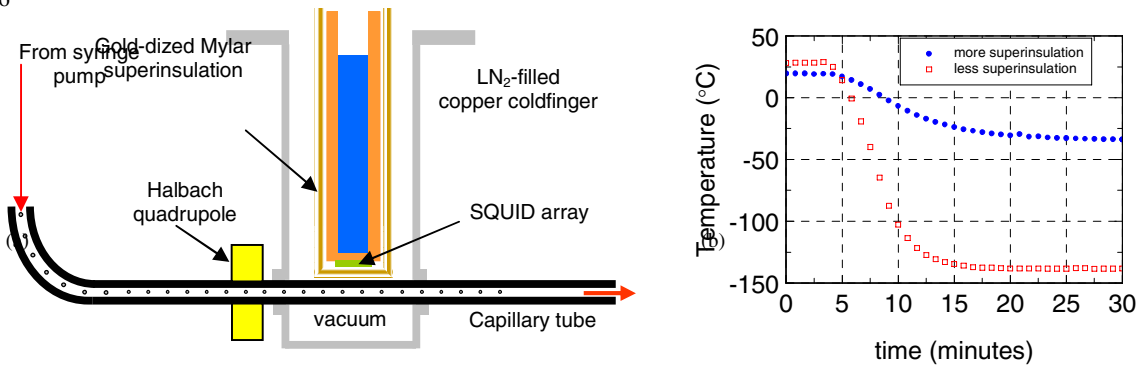


**Figure 2.** (a) Schematic representation of the tail of the magnetic flow cytometer. The SQUID is also surrounded by a mumetal shield (not shown) that clamps on to the tail. In (b) the temperature inside the flow tube (as measured using a thermocouple inside the tube) is shown as a function of superinsulation added. For both cases, PEEK tubing was used.

gradient is removed.

#### 4. Magnetic Flow Cytometer

In this section we describe progress on the SQUID-based detection portion of the magnetic flow cytometer. The tail of the cryogenic dewar, showing the flow tube passing through the vacuum space and the SQUID array on the cold finger, are showing in figure 2(a). Since the signal from a magnetic dipole varies as  $d^3$  (where  $d$  is the distance between the SQUID and the dipole), it is imperative that the sample (flowing at room temperature) is as close as possible to the SQUID array. We have also investigated different materials for the flow tube and also varied the amount of superinsulation surrounding the SQUID. Our initial setup had a titanium tube (1/16" ID) located approximately 1.4 mm below the SQUID with 20 layers of superinsulation around it. In an effort to minimise this lift-off we reduced the number of layers of superinsulation and changed the tube material from titanium to PEEK. The PEEK would complement the other flow system fittings and, while we never expected it to have been a problem before, would not attenuate the signal from the magnetic dipole. However, as shown in figure 2(b) the temperature inside the PEEK tubing became too low, and the flow tube rapidly froze. Adding more superinsulation helped, but not sufficiently to prevent freezing. We subsequently returned to titanium tubing, as the thermal conductivity prevents the freezing behaviour. Unfortunately we were unable to make a temperature measurement with the titanium tube due to the unavailability of such thin gauge, insulated thermocouples (the tube ID is 250  $\mu\text{m}$ ). However, our liftoff measurements indicate a distance from the center of the tube to the SQUIDs of  $\sim 1\text{-}2$  mm and we have plans to reduce this to less than 1 mm. At the same time we will add a solenoid to the tube beneath the SQUIDs (to help magnetize the superparamagnetic particles) and also a thermocouple.

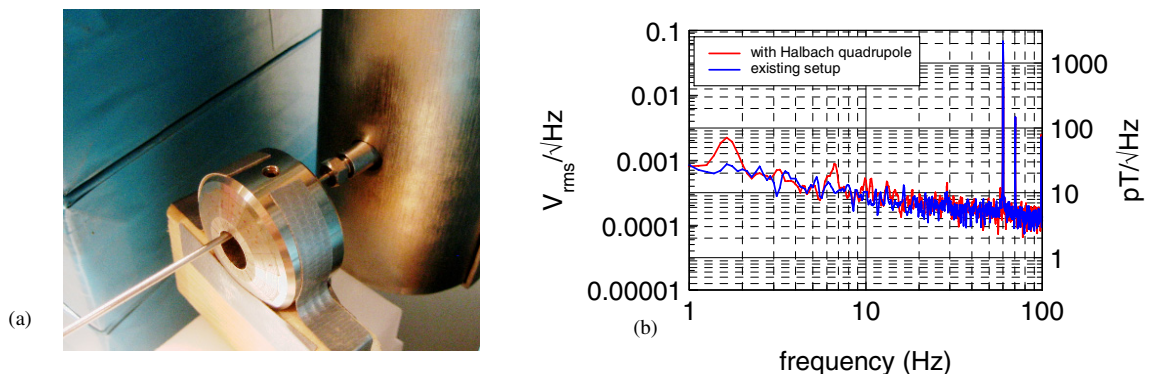


**Figure 3.** (a) Location of the Halbach quadrupole relative to the SQUID array. (b) SQUID noise with and without the quadrupole in position. There is no evidence of Barkhausen noise for  $f > 100$  Hz.

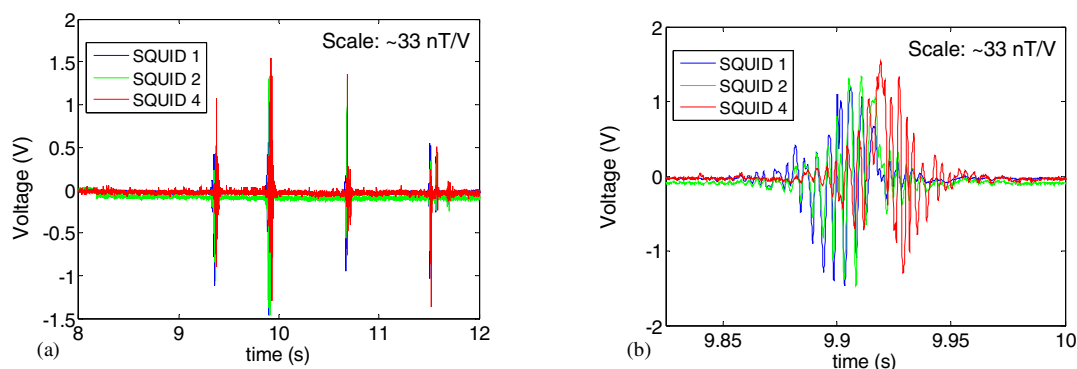


**Figure 4.** (a) The response of 3 SQUIDs in the array to  $\text{SmCo}_5$  flakes. In (b) a more detailed view is given of the 2<sup>nd</sup> event from the left, showing the flake passing under SQUIDs 1, 2 & 4 in that order.

#### 4.1. Detection of Magnetic Particles

Three SQUIDs in the HTS array were used, with their unfiltered flux locked loop output read by the control pc. Post-processing was performed using standard MATLAB routines. Initial tests were performed with magnetic particles glued onto fine gauge wire and pulled through the sample tube by hand. We placed a Halbach quadrupole around the tube outside of the chamber (figure 3(a)) to both magnetize and align the particles. Placing this quadrupole (maximum field 0.46 T) in the vicinity of the SQUID had a negligible effect on the SQUID noise as can be seen in figure 3(b).

Using a water stream, we flowed large  $\text{SmCo}_5$  “flakes” (size  $\sim 50 \mu\text{m}$ ) past the SQUID array and measured the SQUID response using a sampling frequency of 18 kHz. Figure 4(a) shows the response of the 3 SQUIDs to 4 flakes, while in figure 4(b) a more detailed view of one event is shown. Oscillations are, we believe, due to the  $\text{SmCo}_5$  tumbling in flow. The peak to peak amplitude in figure 4(b) corresponds to  $\sim 90 \text{ nT}$ . While the SNR of  $\sim 10:1$  in figure 4 is promising, it is worth noting that we expected signals orders of magnitude greater. From this and other tests it is clear that the magnetic properties of the sample have significantly degraded (due to oxidisation) over the past year.

#### 5. Future Work

The power of this technique is its highly parallel and high throughput nature. Our initial design considerations were based on the availability of polymer-coated  $\text{SmCo}_5$  microspheres. That we have been unable to fabricate such particles has necessarily impinged on both the sorting and the SQUID-based detection. However, we have successfully used commercially available ferromagnetic and superparamagnetic microspheres to demonstrate sorting in proof of principle tests. Improvements in chamber design will further aid the sorting of particles. Decreasing the standoff between the tube and the SQUIDs will help with the SNR, but changing the SQUIDs (to ones with larger effective areas) is an option that may also have to be investigated. We will also incorporate a solenoid around the tube inside the magnetic flow cytometer that will hopefully alleviate the problem of particles becoming demagnetized before they have even reached the SQUID array.

#### Acknowledgment

The authors wish to thank Shaun Newman (Los Alamos National Laboratory) for his technical expertise. This work was funded by the NIH under Grant RR019626-01.

#### References

- [1] Grossman H L *et al* 2004 *PNAS* **101** 129-134
- [2] Ludwig F *et al* 2005 *J. Magn. Magn. Mater.* **293** 690-695
- [3] <http://www.spherotech.com>
- [4] <http://www.bangslabs.com>